

Defects in diamond thin films

M. Fanciulli

Department of Physics, Boston University, Boston, Massachusetts 02215

T. D. Moustakas

*Department of Physics and Department of Electrical, Computer and Systems Engineering,
Boston University, Boston, Massachusetts 02215*

(Received 5 May 1993; revised manuscript received 16 August 1993)

Defects in diamond films, produced by the filament-assisted chemical-vapor deposition of methane and hydrogen as a function of total gas pressure and substrate temperature, were investigated by electron-paramagnetic-resonance measurements. We found an isotropic g value (2.0028 ± 0.0002) independent of growth conditions. The peak-to-peak linewidth increases with pressure from 3.5 to 5 G and the spin density decreases with increasing pressure and temperature and varies between 10^{19} and 10^{17} spins/cm³. The line shape was found to be the superposition of two components, a narrower Lorentzian and a broader Gaussian, suggesting exchange narrowing and a nonuniform distribution of paramagnetic defects. The line shape was analyzed using Van Vleck's theory of moments and a model regarding the distribution of the dominant paramagnetic center in diamond films was proposed and compared with structural studies on the same films. The temperature dependence of the spin-lattice relaxation rate, evaluated by the saturation method, was also investigated.

I. INTRODUCTION

The growth of diamond at low pressures, using vapor-phase deposition methods, is both an interesting problem in the science of crystal growth and a process with significant commercial potential as an alternative to the synthesis of this material by the high-pressure method. Diamond films produced by low-pressure methods are expected to find a large number of applications due to their unique mechanical, thermal, optical and semiconducting properties.

Despite the significant empirical progress in the field of diamond growth, a host of fundamental science problems remains unresolved. Principal among them is the question of diamond nucleation and growth under low-pressure conditions, where diamond should be thermodynamically unstable relative to graphite. One may argue that growth is a nonequilibrium process so equilibrium considerations are not relevant. Thus, a number of groups^{1,2} discussed diamond growth entirely as a kinetic process. Our group has previously observed a qualitative correlation between diamond growth and the existence of defects,^{3,4} and has proposed a quasiequilibrium model⁵⁻⁷ which shows that diamond with a certain concentration of defects is thermodynamically stable over graphite.

Besides any role the defects may play in the stabilization of diamond, their study is important in itself because defects affect the mechanical, thermal, optical, and electronic properties of the material. In many cases, defects in the films are undesirable; however, certain mechanical properties, such as toughness, could improve with certain types of defects. Therefore, the ability to control the defects during film growth and to characterize their nature after film growth is an important area of study. Electron paramagnetic resonance (EPR) is a powerful technique to

study the microstructure of paramagnetic point defects, their interactions with the lattice and their mutual interactions.

Natural and high-pressure synthetic diamond were extensively studied by EPR and excellent review articles were published.⁸ Results were reported on impurities (N or Ni) (Refs. 9 and 10) and paramagnetic centers produced by irradiating the sample with electrons or neutrons^{11,12} or by mechanical damage.¹³ Few studies were presented recently on low-pressure-grown diamond thin films.¹⁴⁻¹⁸

In this paper, we report on a systematic study by EPR of defects in diamond films produced by the hot-filament-assisted chemical-vapor-deposition (CVD) method under various growth conditions. The data are compared with Raman spectroscopy studies which indicate a correlation between defects and diamond growth. A study of the resonance line shape based on the method of moments¹⁹⁻²¹ was carried out and a model regarding the distribution of the dominant paramagnetic center in diamond films was proposed. Spin-lattice relaxation rates have been also investigated as a function of temperature, film morphology, and concentration of defects.

II. EXPERIMENTAL METHODS

The films on which the present study was carried out were prepared by the filament-assisted-CVD method from a gas mixture of CH₄ (2%) and H₂ (98%) with total gas pressure varying from 5 to 75 Torr. The tungsten filament was operated at 1800°C (not corrected for filament emissivity) 10 mm above the substrate which was positively biased relative to the filament. The emission current was held constant at 13 mA/cm² by adjusting the substrate bias voltage. The films were grown on boron-

doped Si(100) substrates roughened by blasting them with SiC powders (25- μm particles). Two series of films, with the substrate temperature at 750 and 950 $^{\circ}\text{C}$ and variable total gas pressure, were grown and investigated. Details on film preparation were published elsewhere.²²

The films were characterized by scanning electron microscopy (SEM), x-ray diffraction (XRD), transmission electron microscopy (TEM), and Raman spectroscopy. XRD studies were performed with Cu $K\alpha$ radiation on diamond films removed from the silicon substrate by dissolving the substrate in acids. TEM studies were performed on thinned diamond samples using the Phillips EM430 electron microscope.²³

EPR measurements were carried out on self-standing diamond films in an X-band Varian E9 spectrometer as a function of temperature using a 100-kHz field modulation and a modulation amplitude of 0.5 G. The g value was evaluated by comparison with a Mn:SrO reference. The absolute number of spins in the samples was obtained by comparison, under the same experimental conditions, with an α, α' -diphenyl- β -picrylhydrazyl (DPPH) reference which was also used as a second reference for the evaluation of the g value. The spin-lattice relaxation time T_{1e} was evaluated from the saturation behavior of the resonance line.²⁴

III. EXPERIMENTAL RESULTS

The surface morphology of the investigated films was found to depend on the total pressure of growth. Films grown at pressures higher than 15 Torr tend to be well faceted, while those grown at lower pressures are less faceted and in some cases have a ball-like morphology. The XRD data are characteristic of polycrystalline diamond films with a lattice constant $a_0 = 3.567 \text{ \AA}$. Bright field TEM images of individual crystals show regions which are largely free of twins and stacking faults and other regions characterized by a high concentration of two families of (111)-type stacking faults.²³ Raman spectroscopy studies on the same samples were reported previously.³ The most important feature from this study is that the Raman line at 1330 cm^{-1} , which is associated with the triply degenerate phonon of F_{2g} symmetry of single-crystal diamond, broadens with reduction of the total pressure of $\text{CH}_4 + \text{H}_2$ without a corresponding shift in frequency. The broadening of the line was attributed to the reduction of the phonon lifetime due to the incorporation of point defects in the films rather than strain. Similar conclusions regarding lack of internal stress in films grown under identical conditions were also reported recently by Gheeraert, Deneuville, and Bonnot.²⁵

All investigated diamond films were found to show a symmetrical resonance line shape which can be deconvoluted into a narrower Lorentzian component and a broader Gaussian component as discussed later. A typical EPR signal is shown in Fig. 1. The summary of the EPR results is presented in Tables I and II for films grown at 750 and 950 $^{\circ}\text{C}$, respectively. We found an isotropic g value of 2.0028 ± 0.002 independent of growth conditions and temperature during the measurements. The linewidth and the concentration of paramagnetic

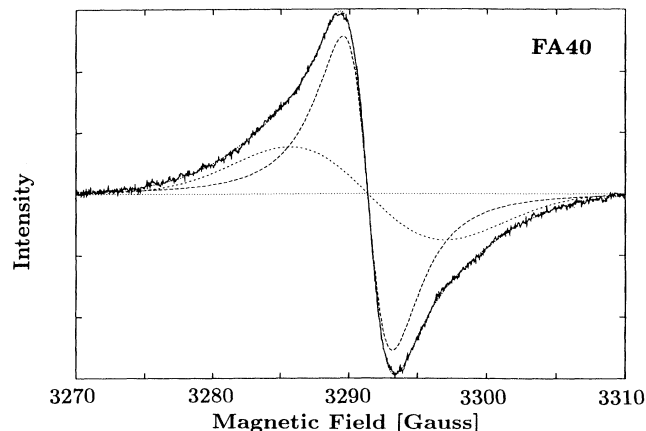


FIG. 1. A typical EPR spectrum (FA40) and best-fit function (—, experimental data; ---, Lorentzian; ···, Gaussian; ····, Lorentzian + Gaussian).

centers were found to depend on the gas pressure and growth temperature as indicated in Figs. 2 and 3, respectively. The data in Fig. 2 show that the peak-to-peak linewidth depends mostly on the gas pressure rather than the substrate temperature. Initially the linewidth increases with the pressure and then saturates at about 5 G. Figure 3 shows that the concentration of spins decreases with increasing gas pressure as well as substrate temperature.

The temperature dependence of the EPR intensity for all the investigated samples was found to satisfy the Curie-Weiss law. This is consistent with electron localization in the defect and rules out contribution to the signal from conduction electrons in graphitic regions.

The spin-lattice relaxation rate T_{1e}^{-1} was found to depend on the morphology of the films. Thus the values of T_{1e}^{-1} were evaluated as a function of temperature for one film with ball-like morphology (FA44) and another with faceted morphology (FA40). The results are reported in Fig. 4. Both samples show an almost temperature-independent spin-lattice relaxation rate for $T < 100 \text{ K}$. At higher temperature the spin-lattice relaxation rate can be described by the relation T^α where $\alpha \approx 3$ for the sample with ball-like morphology and $\alpha \approx 5$ for the sample with faceted morphology. In the whole investigated temperature range we found $T_{1e, \text{FA44}} < T_{1e, \text{FA40}}$.

IV. DISCUSSION

A. Line shape and distribution of defects

The shape of the resonance line was analyzed for three samples having peak-to-peak linewidth of 3.5, 4.5, and 5 G. The resonance line was deconvoluted into a Lorentzian and a Gaussian component, as shown in Fig. 1, using a nonlinear best fit based on the Marquardt method.²⁶ The fitting function is given by

$$Y'(H) = Y'_{\text{Lor}} + Y'_{\text{Gauss}}, \quad (1)$$

where

TABLE I. Growth conditions and experimental results for the samples grown at 750°C.

Sample	Total pressure (Torr)	<i>g</i> value	ΔH_{pp} (G)	N_{exp} (spins/cm ³)
FA44	5	2.0028±0.0002	3.5±0.5	1.8×10 ¹⁹
FA42	15	2.0028±0.0002	4.0±0.5	1.3×10 ¹⁹
FA40	25	2.0028±0.0002	4.5±0.5	5.9×10 ¹⁸
FA41	75	2.0028±0.0002	4.5±0.5	4.9×10 ¹⁸

$$Y'_{Lor} = \frac{16y'_{max,Lor} [(H-H_0)/\frac{1}{2}\Delta H_{pp,Lor}]}{\{3 + [(H-H_0)/\frac{1}{2}\Delta H_{pp,Lor}]^2\}^2}, \quad (2)$$

$$Y'_{Gauss} = y'_{max,Gauss} \left[\frac{H-H_0}{\frac{1}{2}\Delta H_{pp,Gauss}} \right] \times \exp \left\{ -\frac{1}{2} \left[\left[\frac{H-H_0}{\frac{1}{2}\Delta H_{pp,Gauss}} \right]^2 - 1 \right] \right\}. \quad (3)$$

The parameters of the fitting are reported in Table III. The center field H_0 was found to be the same for the two components indicating a common nature of the paramagnetic centers responsible for the two lines. Listed in Table III are also the ratio of the Lorentzian component and Gaussian component areas versus the total area of the line. Similar results were obtained using the linear anamorphosis method.²⁷ Note that the Lorentz contraction becomes less and less important as a function of the total growth pressure. The second (M_2) and fourth (M_4) moments of the resonance line were evaluated from the fitting function where the Lorentzian contribution was limited to the range $|H-H_0| \leq 40$ G. The ratio $M_4/3M_2^2$, which is expected to be 1 for a pure Gaussian and increases as the Lorentzian component becomes dominant, can be considered as measure of the narrowing. The results of this calculation are also reported in Table III.

The analysis of the line shape shows that the wings of the line profile have Gaussian character while the center has a Lorentzian form. Broadening effects due to strain in the films have been ruled out based on Raman spectroscopy studies done on the same films³ as previously discussed. It is known that a weak dipole-dipole interaction broadens the EPR spectra²⁸ while exchange interaction of like paramagnetic centers leads to a narrowing of the line shape.¹⁹ The existence of a spectrum with narrow and broad lines is consistent with the presence, in the same sample, of regions characterized by a higher concentration of paramagnetic centers in addition to regions with a lower concentration of the same centers. The overall line shape is due to the fact that the concentration

of paramagnetic centers in a certain volume of the crystal attains a value such that the dipole-dipole interaction of the unpaired spins of neighboring centers is already pronounced (Gaussian broadening) and exchange interaction becomes significant (Lorentz contraction of the lines). Therefore, in the attempt of explaining the observed line shape, the following Hamiltonian has to be considered:¹⁹⁻²¹

$$\mathcal{H} = \mathcal{H}_{Ze} + \mathcal{H}_{exc} + \mathcal{H}_{dip}, \quad (4)$$

where \mathcal{H}_{Ze} , \mathcal{H}_{exc} , and \mathcal{H}_{dip} are the electron Zeeman, exchange, and dipolar interaction terms,

$$\mathcal{H}_{Ze} = Hg\beta \sum_j S_{z_j}, \quad (5)$$

$$\mathcal{H}_{exc} = \sum_{k>j} \tilde{A}_{jk} \mathbf{S}_j \cdot \mathbf{S}_k, \quad (6)$$

$$\mathcal{H}_{dip} = g^2\beta^2 \sum_{k>j} [r_{jk}^{-3}(\mathbf{S}_j \cdot \mathbf{S}_k) - 3r_{jk}^{-5}(\mathbf{r}_{jk} \cdot \mathbf{S}_j)(\mathbf{r}_{jk} \cdot \mathbf{S}_k)]. \quad (7)$$

In these expressions g is the g value, β is the Bohr magneton, S_{z_j} is the z component of the spin of the unpaired electron on the j th site, $\mathbf{S}_j, \mathbf{S}_k$ are the spins of unpaired electrons on the j th and k th paramagnetic center, r_{jk} is the distance between these centers, $\tilde{A}_{jk} = 2z^2 J_{jk}$ (z is the number of unpaired electrons in the center and J_{jk} is the exchange integral). Using the method of moments the concentration and distribution of paramagnetic centers and the magnitude of the exchange interaction energy can be obtained. The second and fourth moments of the absorption line for a polycrystalline material (averaging with respect to all direction) are^{19,20}

$$M_2 = \frac{3}{5}g^2\beta^2 S(S+1) \sum_{k'} r_{jk'}^{-6}, \quad (8)$$

$$M_4 = 3(1-\eta)M_2^2 + \frac{6}{5}\tilde{A}^2 S^2(S+1)^2 \sum_{k'} r_{jk'}^{-6}, \quad (9)$$

TABLE II. Growth conditions and experimental results for the samples grown at 950°C.

Sample	Total pressure (Torr)	<i>g</i> value	ΔH_{pp} (G)	N_{exp} (spins/cm ³)
FA52	5	2.0028±0.0002	3.5±0.5	2.5×10 ¹⁸
FA53	15	2.0028±0.0002	3.5±0.5	1.5×10 ¹⁸
FA48	30	2.0029±0.0002	5.0±0.5	3.2×10 ¹⁷
FA50	60	2.0028±0.0002	5.0±0.5	1.9×10 ¹⁷

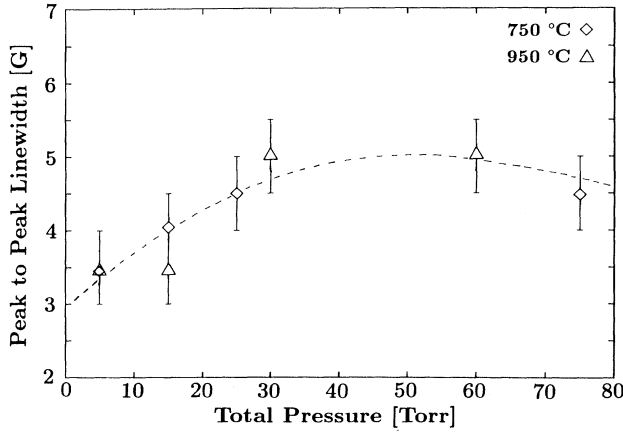


FIG. 2. Peak-to-peak linewidth as a function of total gas pressure and temperature.

where

$$\eta = \frac{2}{9} + \frac{1}{7} \frac{\sum_{k'} r_{jk'}^{-12}}{\left[\sum_{k'} r_{jk'}^{-6} \right]^2} \left[\frac{58}{9} + \frac{3}{2S(S+1)} \right]. \quad (10)$$

In Eqs. (8), (9), and (10) S is the effective spin of the center which is assumed to be $S = \frac{1}{2}$. The term in Eq. (9) containing the exchange interaction was computed considering only adjacent paramagnetic centers and assuming $\bar{A}_{jk} = \bar{A}$ since the exchange interaction decreases very rapidly with distance. The sums in Eqs. (8), (9), (10) are taken over all sites of the diamond crystal structure occupied by a paramagnetic center ($\sum_{k'}$). To compute these sums we consider two different models for the distribution of paramagnetic centers.

In the first model we assume a random distribution of paramagnetic centers with uniform probability f that a lattice site is occupied by a magnetic system.²⁹ In this case we have

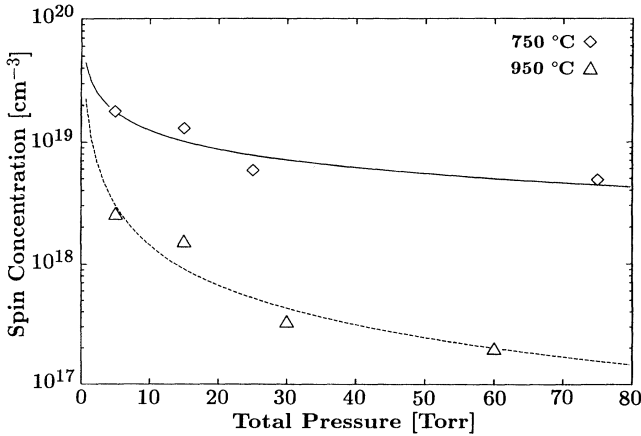


FIG. 3. Concentration of paramagnetic centers as a function of total gas pressure and temperature.

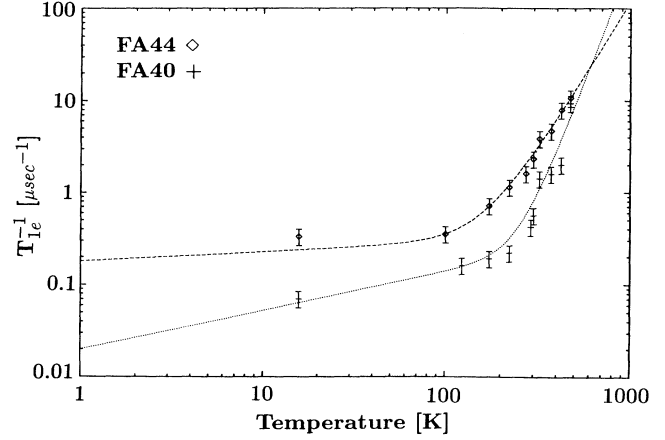


FIG. 4. Spin-lattice relaxation rates for samples FA44 and FA40.

$$\sum_{k'} r_{jk'}^{-6} = f \sum_k r_{jk}^{-6} = f \delta a_0^{-6}, \quad (11)$$

where the second sum in Eq. (11) is over all sites of the diamond crystal structure and a_0 is the lattice constant. The constant δ was calculated considering 5850 neighbors ($r_{jk} < \sqrt{499/16}a_0$) and was found to be $\delta = 776.05$ (the sum converges very rapidly and actually only a few coordination spheres contribute significantly to the final value). Similarly, the sum $\sum_{k'} r_{jk'}^{-12}$ was calculated to be $f \delta' a_0^{-12}$ with $\delta' = 92951.34$. Using Eq. (8), Eq. (11), and the experimental values of M_2 , from Table III, we calculated the values for the probability f . For the investigated samples f was found to have the following values: $f_{FA44} = 4.88 \times 10^{-7}$, $f_{FA40} = 5.52 \times 10^{-7}$, $f_{FA50} = 6.28 \times 10^{-7}$. From these values a spin density 1–2 orders of magnitude lower than the experimental values have been calculated for samples FA44 and FA40. For sample FA50 the agreement with the experimental value is good, but in general such a low concentration of defects cannot account for the observed line shape. Therefore this model is not consistent with our experimental results.

An alternative model is to consider a dilute magnetic lattice that is an expanded diamond crystal structure where all sites are occupied by a paramagnetic center. In this case we have

TABLE III. Parameters related to the line shape for samples FA44, FA40, and FA50.

	FA44	FA40	FA50
$\Delta H_{pp, \text{exp}}$ (G)	3.5	4.5	5.0
$\Delta H_{pp, \text{Lor}}$ (G)	3.2	3.7	3.5
$y_{\text{max, Lor}}$ (a.u.)	1538.96	1277.37	522.96
$\Delta H_{pp, \text{Gauss}}$ (G)	10.9	11.3	13.4
$y'_{\text{max, Gauss}}$ (a.u.)	196.37	379.89	184.17
$A_{\text{Lor}}/A_{\text{exp}}$	0.70	0.55	0.40
$A_{\text{Gauss}}/A_{\text{exp}}$	0.3	0.45	0.60
M_2 (G ²)	28.9	32.7	37.2
M_4 (G ⁴)	3494.5	3936.6	4499.1
$M_4/3M_2^2$	1.40	1.23	1.08

$$\sum_{k'} r_{jk'}^{-6} = \sum_k \bar{r}_{jk}^{-6} = \delta d_0^{-6}, \quad (12)$$

where d_0 is the lattice constant of the dilute lattice described by the coordinates \bar{r}_{jk} . From Eq. (8) and Eq. (12) we can evaluate d_0 and therefore the concentration of paramagnetic centers. The values of d_0 , the distances between first neighbors \bar{r} , and the calculated concentration of paramagnetic centers N_1 are reported in Table IV. N_1 is one to three orders of magnitude larger than the experimental value N_{exp} . This discrepancy could be eliminated if we assume a nonuniform distribution of paramagnetic defects in the samples. The experimental concentration is an average value over the total volume of the sample which is in reality characterized by a fraction of its volume (V_1/V) with a higher concentration of spins (N_1) and the rest with a lower concentration of spin (N_2). Relating the calculated total number of defects to the Gaussian component A_G (the second moment is unaffected by exchange interaction) and the experimental total number of defects to the experimental line A_{exp} we can evaluate the fraction of volume with the higher concentration of spins as

$$\frac{V_1}{V_{\text{tot}}} \sim \frac{A_G N_{\text{exp}}}{A_{\text{exp}} N_1}. \quad (13)$$

The results of this analysis are reported in Table IV.

The narrowing of the linewidth with the decreasing of the pressure, shown in Fig. 1, is then interpreted as due to exchange interaction in the region with higher defect concentration. The volume of these regions was found to be larger for films grown at lower pressures. This explains why exchange narrowing appears in both sets of films grown at 750 and 950°C even though the concentration of defects for the latter set is one order of magnitude smaller than the former.

Under the assumption of dilute magnetic lattice we evaluate the exchange energy from the experimental second and fourth moments of the resonance line. From Eq. (8) and Eq. (9) we have

$$\bar{A}^2 = \frac{M_4 - 3M_2^2(1-\eta)}{2S(S+1)M_2} \frac{g^2\beta^2}{h^2c^2}. \quad (14)$$

A value of $\bar{A} \sim 6 \times 10^{-4} \text{ cm}^{-1}$ was found for the three analyzed samples. A similar result ($\bar{A} \sim 3.5 \times 10^{-4} \text{ cm}^{-1}$ for $r \sim 22 \text{ \AA}$) was obtained for nonuniformly distributed substitutional nitrogen in polycrystalline synthetic diamond.²⁰ The lack of hyperfine or superhyperfine interac-

tions, and therefore the lack of information regarding the defect wave function, does not allow us to perform a theoretical estimation of the exchange energy as a function of distance between the paramagnetic centers. This calculation was performed for substitutional nitrogen³⁰ and the theoretical result was found to be in good agreement with the value obtained using the experimental results and Van Vleck's theory.²⁰

Alternatively one may consider a Gaussian discrete distribution of d_0 , a Gaussian discrete distribution of the distance $r_{jk'}$ between the paramagnetic centers, or a more general probability function. However, the main conclusion, related to the nonuniform distribution of defects, the existence of close pairs responsible for the exchange narrowing, and the temperature dependence of the spin-lattice relaxation rate, as discussed later, is not expected to be modified.

B. Nature of the defect

The observed g value of 2.0028 ± 0.0002 is consistent with the A center first observed by Griffiths, Owen and Ward¹¹ and then by Faulkner and Lomer¹² on neutrons and electrons irradiated type-IIA diamond, respectively. In addition to the central line, this center shows satellite lines which, depending on the irradiation dose, may or may not be resolved. A number of groups speculated as to the nature of this center. O'Brien and Pryce³¹ suggested vacancies and interstitial carbon atoms as being responsible for this center. Yamaguchi,³² whose calculations have shown that the negatively charged vacancy V^- is the dominant defect with ground state 4A and the first excited state 2T , suggested that V^- is related to this A center. Harris, Owen, and Windsor³³ proposed, following this suggestion, that the pair of satellite lines observed in the spectrum may be due to the splitting of the $S = \frac{3}{2}$ spin levels via lattice distortion by a neighboring diamagnetic interstitial atom C^0 . The nondegenerate state 4A has been recently demonstrated, by EPR and electron-nuclear double-resonance measurements,³⁴ to be the ground state of the negatively charged vacancy. Walter and Estle¹³ observed a single-line EPR spectrum with a g value of 2.0027 ± 0.0008 and a peak-to-peak linewidth of 5–6 G from crushed diamond.

The identification of the main paramagnetic center as being the negatively charged vacancy in the set of investigated films is consistent with our EPR results. However, positron annihilation measurements, reported by Dannefaer, Bretagnon, and Kerr,³⁵ exclude the presence, to within the experimental sensitivity (~ 0.2 ppm), of charged states of the single vacancy. Based on the positron lifetime, these authors derived a concentration of vacancy clusters (~ 6 vacancies) of the order of 10^{18} cm^{-3} .

Based on our results and on the positron annihilation measurements, we suggest that the region of high concentration of paramagnetic centers could be either dangling bonds in multivacancies or in areas which show extensive concentration of (111) stacking faults. The region of low concentration of EPR centers could be related to dangling bonds distributed throughout the material in smaller multivacancies or dislocations.

TABLE IV. Parameters related to the evaluated distribution of paramagnetic centers for the samples FA44, FA40, and FA50.

	FA44	FA40	FA50
d_0 (Å)	40.12	39.31	38.47
\bar{r} (Å)	17.37	17.02	16.66
N_{exp} (cm^{-3})	1.8×10^{19}	5.9×10^{18}	1.9×10^{17}
N_1 (cm^{-3})	1.2×10^{20}	1.3×10^{20}	1.4×10^{20}
V_1/V_{tot} (%)	4.2	2.0	0.08
N_2 (cm^{-3})	1.4×10^{19}	3.4×10^{18}	7.8×10^{16}

C. Spin-lattice relaxation rate

The experiments show an increase in the relaxation rate T_{1e}^{-1} with increasing spin concentration. This suggests the influence of some rapidly relaxing center characterized by a strong spin-phonon interaction. These centers could be groups of closely situated paramagnetic defects between which considerable exchange interaction acts³⁶ [$A(r) \gg A(\bar{r})$ where $\bar{r} \sim 17 \text{ \AA}$ is the distance from the evaluated concentration]. The assumption $\mathcal{H}_{\text{exc}} \gg \mathcal{H}_{\text{Ze}}$ is consistent with relaxation by conversion into exchange energy and then through the dipolar interaction into one or two lattice phonons.³⁷ This assumption cannot explain the observed temperature dependence of the relaxation rates.^{38,39} However, even if $\mathcal{H}_{\text{exc}} \ll \mathcal{H}_{\text{Ze}}$ (in agreement with the evaluated exchange energy) and the exchange interaction is not considered an individual reservoir the spin-lattice relaxation rate of the Zeeman subsystem to the lattice could be significantly affected. It was shown by Buishvili and Khalvashi⁴⁰ that, if the spin-lattice interaction operator does not commute with the exchange interaction, the relaxation rate depends on the concentration N and on the temperature as

$$T_{1e}^{-1} \propto NT^m, \quad (15)$$

where m is 3 or 5 depending on the specific relaxation mechanism (direct or Raman process, respectively). This analysis could explain the experimental results at temperatures higher than 100 K. The fact that the direct process dominates in the sample with ball-like morphology may be attributed to an increase of the phonon spectral density at low energies due to disorder. The most temperature-independent relaxation rate at temperatures lower than 100 K could be related to spin-spin interaction. In this case the recovery could be due to the transfer of excitation by a temperature-independent spin-spin process in which pairs for which $r \ll \bar{r}$ and so $A(r) \gg A(\bar{r})$ constitute an independent reservoir. Such a process should be dependent on the concentration of paramagnetic centers, as we observed, and practically independent of the field H . Honig,^{41,42} on the basis of Bloembergen's analysis of nuclear relaxation by paramagnetic impurities,⁴³ outlined a model to explain the concentration-dependent relaxation process in n -type silicon. In this model the isolated spins relax via spin diffusion to fast-relaxing centers consisting of pairs arising because of the nonuniform distribution of the centers. A more detailed analysis of our results based on this model will be the subject of a future study.⁴⁴ Results qualitatively similar to those reported were obtained on samples containing nitrogen-vacancy and nitrogen-divacancy complexes.⁴⁵

D. Film growth

The trend in the concentration of the paramagnetic defects, shown in Fig. 3, as well as the trend in the Raman spectra and the morphological changes, suggest that the reduction of gas pressure during diamond growth by the filament-assisted CVD process increases the concentration of defects in the films. We believe that lattice defects

(vacancies) are introduced in the films by atomic hydrogen etching of carbon atoms and incomplete subsequent regrowth.⁶ Atomic hydrogen becomes a more efficient etchant at the lowest pressure because its mean free path and its recombination lifetime are higher at the lowest pressures.⁴⁶

The observed decrease of paramagnetic defects with increase in substrate temperature (see Fig. 3) suggests a partial annealing of defects with growth temperature. Some vacancies may anneal out by migrating to the surface and others may cluster to form large multivacancies.

These data are in qualitative agreement with the model on defect-induced stabilization of diamond over graphite proposed by Bar-Yam and Moustakas.^{5,6} In this model the incorporation of certain defects during diamond film growth reverses the thermodynamic stability between diamond and graphite. The formations of vacancies as well as the growth rate of the films are determined by carbon etching processes. For example, the commonly observed growth rate of $1 \mu\text{m/h}$ (or 1.5 monolayers/sec) requires the deposition of 10^{15} carbon atoms/cm² sec on the substrate. However, the deposition rate from a 100-Torr mixture of hydrogen with 1% CH₄ is expected to be 10^{21} carbon atom/cm² sec (or 10^6 monolayers/sec). Thus the diamond growth should be understood as a multiple regrowth process, i.e., many layers are grown and removed for each layer ultimately deposited. This rapid growth and regrowth process leads to materials with large concentration of vacancies. These vacancies are likely to cluster and form multivacancies which are more stable at the high temperatures of growth. Thus, this model of growth is consistent qualitatively with the observed EPR defects being dangling bonds in internal surfaces of multivacancies.

V. CONCLUSIONS

In conclusion, diamond films, produced by the filament-assisted CVD process, were found to have a concentration of paramagnetic centers in the range 10^{17} – 10^{19} cm⁻³ with an isotropic g value of 2.0028 independent of growth conditions. A defect with such a g value is consistent with either a negatively charged vacancy or a dangling bond in multivacancies or dislocations. The analysis of the line shape using Van Vleck's theory of moments is consistent with a nonuniform distribution of the EPR centers in the diamond films. More specifically, the majority of defects are clustered in a very small volume fraction of the sample, while the rest of the sample contains a smaller concentration of the same defects. The clustered defects are assumed to be dangling bonds in large multivacancies or regions with an extensive concentration of (111) stacking faults, while the distributed defects are assumed to be dangling bonds in smaller multivacancies or dislocations.

The spin-lattice relaxation rate was found to depend on the temperature, the concentration of defects, and the film morphology. The almost temperature-independent spin-lattice relaxation rate at low temperatures was attributed to a spin-diffusion process to rapidly relaxing close pairs of paramagnetic centers. At higher temperatures

the spin-lattice relaxation rate temperature dependence was found to be consistent with direct or Raman relaxation processes where the spin-lattice operator does not commute with the exchange Hamiltonian and the exchange interaction is not considered an independent reservoir.

The dependence of the concentration of paramagnetic defects on pressure during film growth was found to be in qualitative agreement with Raman spectra and morphological changes in the films. The data suggest that diamond growth at lower pressures introduces more defects in the films due to atomic hydrogen etching of carbon atoms and subsequent incomplete overgrowth. The same

trends are also qualitatively consistent with the model of defect-induced stabilization of diamond under metastable conditions.

ACKNOWLEDGMENTS

This research was supported by the National Science Foundation (Grant No. DMR-9014370). We would like to thank Professor E. R. Weber and Dr. P. Dreszer of the University of California at Berkeley for stimulating discussions. We are also indebted to Professor Hans van Willigen of the University of Massachusetts for the use of the EPR facilities.

- ¹M. Tsuda, M. Nakajima, and S. Oikawa, *J. Am. Chem. Soc.* **108**, 5780 (1986).
- ²D. Huang, M. Frenklach, and M. Maroncelli, *J. Phys. Chem.* **92**, 6379 (1988); M. Frenklach and K. Spear, *J. Mater. Res.* **3**, 133 (1988).
- ³R. G. Buckley, T. D. Moustakas, Ling Ye, and J. Varon, *J. Appl. Phys.* **66**, 3595 (1989).
- ⁴R. J. Graham, T. D. Moustakas, and M. M. Disko, *J. Appl. Phys.* **69**, 3212 (1991).
- ⁵Y. Bar-Yam and T. D. Moustakas, *Nature (London)* **342**, 786 (1989).
- ⁶Y. Bar-Yam and T. D. Moustakas, in *Diamond, Silicon Carbide and Related Wide Bandgap Semiconductors*, edited by J. T. Glass, R. F. Messier, and N. Fujimori, MRS Symposia Proceedings No. 162 (Materials Research Society, Pittsburgh, 1990), p. 201.
- ⁷T. D. Moustakas, in *Synthetic Diamond: Emerging CVD Science and Technology*, edited by K. E. Spear and J. P. Dismukes (Wiley, New York, 1993).
- ⁸J. H. Loubser and J. A. Van Wyk, *Rep. Prog. Phys.* **41**, 1201 (1978).
- ⁹W. V. Smith, P. P. Sorokin, I. L. Gelles, and G. J. Lasher, *Phys. Rev.* **115**, 1546 (1959).
- ¹⁰J. H. N. Loubser and W. P. van Ryneveld, *Nature (London)* **211**, 517 (1966).
- ¹¹J. H. E. Griffiths, J. Owen, and I. M. Ward, *Rep. Conf. Defects in Crystalline Solids* (Physical Society, London, 1955), p. 81.
- ¹²E. A. Faulker and J. N. Lomer, *Philos. Mag.* **7**, 1995 (1962).
- ¹³G. K. Walter and T. L. Estle, *J. Appl. Phys.* **32**, 1854 (1961).
- ¹⁴I. Wantanabe and K. Sugata, *Jpn. J. Appl. Phys.* **27**, 1808 (1988).
- ¹⁵M. Hoikins, E. R. Weber, M. I. Laundstrass, M. A. Plano, S. Han, and D. R. Kania, *Appl. Phys. Lett.* **59**, 1871 (1991).
- ¹⁶M. Fanciulli and T. D. Moustakas, *Diamond Relat. Mater.* **1**, 773 (1992).
- ¹⁷M. Fanciulli, S. Jin, and T. D. Moustakas, *Bull. Am. Phys. Soc.* **37**, 710 (1992).
- ¹⁸M. Fanciulli and T. D. Moustakas, *Physica B* **185**, 228 (1993).
- ¹⁹J. H. Van Vleck, *Phys. Rev.* **74**, 1168 (1948).
- ²⁰L. A. Shul'man and G. A. Podzyarei, *Teor. Eksp. Khim.* **1**, 830 (1965).
- ²¹N. D. Samsonenko, *Fiz. Tverd. Tela (Leningrad)* **6**, 3086 (1965) [*Sov. Phys. Solid State* **6**, 2460 (1965)].
- ²²T. D. Moustakas, *Solid State Ion.* **32-33**, 861 (1989).
- ²³M. M. Disko and T. D. Moustakas, in *Characterization of the Structure and Chemistry of Defects in Materials*, edited by B. C. Larson, M. Rühle, and D. N. Seidman, MRS Symposia Proceedings No. 138 (Materials Research Society, Pittsburgh, 1989), p. 261.
- ²⁴C. P. Poole, Jr., *Electron Spin Resonance*, 2nd ed. (Wiley, New York, 1983).
- ²⁵E. Gheeraert, A. Deneville, and A. M. Bonnot, *Diamond Relat. Mater.* **1**, 525 (1992).
- ²⁶D. W. Marquardt, *J. Soc. Ind. Appl. Math.* **2**, 431 (1963).
- ²⁷N. N. Tikhomirova and V. V. Voevodskii, *Opt. Spektrosk* **7**, 829 (1959).
- ²⁸M. H. Pryce and K. W. H. Stevens, *Proc. Phys. Soc. London, Ser. A* **63**, 36 (1950).
- ²⁹C. Kittel and E. Abrahams, *Phys. Rev.* **90**, 238 (1953).
- ³⁰L. A. Shul'man, I. M. Zaritskii, and K. A. Tikhonenko, *Fiz. Tverd. Tela (Leningrad)* **9**, 1964 (1968) [*Sov. Phys. Solid State* **9**, 1545 (1968)].
- ³¹M. C. M. O'Brien and M. H. L. Pryce, *Rep. Conf. Defects in Crystalline Solids* (Ref. 11), p. 88.
- ³²T. Yamaguchi, *J. Phys. Soc. Jpn.* **17**, 1359 (1962).
- ³³E. A. Harris, J. Owen, and C. Windsor, *Bull. Am. Phys. Soc.* **8**, 252 (1963).
- ³⁴J. Isoya, H. Kanda, Y. Uchida, S. C. Lawson, S. Yamasaki, H. Itoh, and Y. Morita, *Phys. Rev. B* **45**, 1436 (1992).
- ³⁵S. Dannefaer, T. Bretagnon, and D. Kerr (unpublished).
- ³⁶J. H. Van Vleck, *Quantum Electronics* (Columbia University Press, New York, 1960), p. 392.
- ³⁷N. Bloembergen and S. Wang, *Phys. Rev.* **93**, 72 (1954).
- ³⁸R. B. Griffiths, *Phys. Rev.* **124**, 1023 (1961).
- ³⁹P. M. Richards, *Phys. Rev.* **137**, A1327 (1965).
- ⁴⁰L. L. Buishvili and K. H. Khalvashi, *Phys. Status Solidi B* **55**, K13 (1973).
- ⁴¹A. Honig and E. Stupp, *Phys. Rev.* **117**, 69 (1960).
- ⁴²G. Yang and A. Honig, *Phys. Rev.* **168**, 271 (1968).
- ⁴³N. Bloembergen, *Physica (Utrecht)* **15**, 386 (1949).
- ⁴⁴M. Fanciulli (unpublished).
- ⁴⁵I. M. Zaritskii, V. Ya. Bratus', V. S. Vikhnin, A. S. Vishnevskii, A. A. Konchits, and V. M. Ustintsev, *Sov. Phys. Solid State* **18**, 1183 (1977).
- ⁴⁶T. R. Anthony, in *Diamond and Diamond-like Films and Coatings*, NATO Advanced Study Institute on Diamond and Diamond-like films, edited by R. E. Clausing (Plenum, New York, 1991).